

# Thickness dependent aggregation of Fe–silicide islands on Si substrate

G. Molnár\*, L. Dózsa, G. Petó, Z. Vértesy, A.A. Koós, Z.E. Horváth, E. Zsoldos

MTA Research Institute for Technical Physics and Materials Science, H-1525 Budapest, P.O. Box 49, Hungary

Available Online February 26 2004

## Abstract

Iron–silicides were grown on Si by reactive deposition epitaxy method and by conventional solid phase reaction. The morphology of silicides was investigated by optical microscopy, scanning electron microscopy and by atomic force microscopy. The phases formed were identified by X-ray diffraction. The thickness of the evaporated Fe films ranged from 1.5 to 30 nm and the in situ heat treatments were carried out between 500 and 800 °C. Self-assembled, island like, oriented  $\beta$ -FeSi<sub>2</sub> and  $\alpha$ -FeSi<sub>2</sub> were found to grow on Si(100) substrates under 15 nm initial Fe thickness. The size of the islands was between 20 and 500 nm, and their shape varied from circular to faceted triangular and quadratic depending on the Fe thickness and on the annealing. Above 20 nm evaporated Fe thickness, the samples show islands of  $\beta$ -FeSi<sub>2</sub> phase grown into the FeSi matrix indicating a nucleation controlled type transition of the FeSi to  $\beta$ -FeSi<sub>2</sub> phase.

© 2003 Elsevier B.V. All rights reserved.

PACS: 81.16.Dn; 68.55-a

Keywords: Iron–silicide; Self-assembly; Epitaxy

## 1. Introduction

Thin films of metal silicides have attracted attention because of their scientific curiosity and technical importance. They have generally metal like electrical resistivity, and exhibit good high temperature stability and oxidation resistance [1]. The silicides can be classified, for example according to their formation kinetics from a metallic thin film and silicon substrate conventional solid phase reaction. The most important type of kinetics is the group of diffusion-controlled reactions. All diffusion-controlled reactions have an initial stage under a certain thickness, where they exhibit reaction controlled growth kinetics [2]. The next category of kinetics, the nucleation controlled reactions occur where nucleation is so difficult that it dominates the process of phase formation [3].

$\beta$ -FeSi<sub>2</sub> is an indirect semiconductor, but in some epitaxial configurations on silicon substrate it has a direct band gap due to strain effects [4–6]. For this reason, it is a potential material of optoelectronic applications in silicon-integrated technology. A lot of effort

has been made to prepare semiconducting epitaxial  $\beta$ -FeSi<sub>2</sub> layers, whilst less work has been done to understand the basic solid phase reaction of Fe thin film and Si substrate. According to the literature [Refs. [7–10]], the following phases of the Fe–Si equilibrium phase diagram have found in thin film reactions, mainly on Si(111) substrates: The most Fe-rich silicide is Fe<sub>3</sub>Si (DO<sub>3</sub> type), with cubic structure. Two types of iron monosilicides may appear in thin film form. The first phase is  $\epsilon$ -FeSi with cubic structure and the second monosilicide phase is cesium–chloride type cubic FeSi. The iron disilicides, prepared in thin layers, might have three different crystal structures. The high temperature, metastable, tetragonal  $\alpha$ -FeSi<sub>2</sub> phase may be epitaxially stabilized in thin film form on Si substrates. The cubic  $\gamma$ -FeSi<sub>2</sub> phase is also a metastable structure. At the end,  $\beta$ -FeSi<sub>2</sub> has orthorhombic structure. All of the above phases, including metastable ones, may be epitaxially stabilized on the surface of Si(111) substrates.

The preparation of artificial low dimensional structures for electron confinement is one of the most challenging research fields of the solid-state technology [11]. The phenomena of self-assembly have been observed besides compound and group IV semiconductors in a wide range of material and substrate combina-

\*Corresponding author. Tel.: +36-1-3922236; fax: +36-1-3922226.

E-mail address: [molnargy@mfa.kfki.hu](mailto:molnargy@mfa.kfki.hu) (G. Molnár).

tions [12]. Heteroepitaxial growth of strained semiconductor structures has attracted great interest recently, owing to their scientific curiosity and possible technical importance as quantum dots [13]. The generated dots, through the combination of growth kinetics and strain effects show a rather narrow size distribution on the top of their substrate.

Earlier, a few publications reported island or wire likes aggregation of the silicides on Si substrates.  $\text{TiSi}_2$  islands were observed both on Si(100) and Si(111) by Ti deposition at elevated temperatures followed by high temperature annealing [14].  $\text{CoSi}_2$  nanostructures were prepared on Si(100) by reactive deposition epitaxy (RDE) and their nucleation and evolution were studied during the annealing [15]. Recently, two groups in case of the rare earth (Er, Dy, Ho) silicides [16,17] reported nanowire formation.

Suemasu and coworkers reported first the aggregation of monocrystalline  $\beta\text{-FeSi}_2$  islands on the top of Si(100) substrate and the spherical transformation of islands inside a Si overlayer [18].

The motivation of the recent study was to demonstrate the possibility of self assembled island formation of epitaxial Fe–silicides on Si(100) substrates, with the long term plan to develop epitaxial, semiconductive  $\beta\text{-FeSi}_2$  quantum dots on the surface of Si. We investigated the thickness interval, where the stress effects play important role during the solid phase reactions, namely, between the monolayer and 20–30 nm coverage. The evolution of aggregated silicide was followed as a function of the annealing temperature and time and initial iron film thickness.

## 2. Experimental

Pieces of n-type (100) oriented Si wafers were used as substrates. Before loading the samples into the oil free evaporation chamber, their surface was refreshed in diluted HF. The time elapsed after cleaning to reach 1 Pa pressure in the vacuum chamber was approximately 30 min. After evacuation down to  $1 \times 10^{-6}$  Pa and prior to evaporation, Si wafers were annealed in situ for 5 min at 800 °C. Iron ingots of 99.9% purity were evaporated using an electron gun, at an evaporation rate of 0.01–0.03 nm/s, at a pressure of  $3 \times 10^{-6}$  Pa. The film thickness was measured by vibrating quartz. The major parts of the samples were prepared by reactive deposition epitaxy method (RDE), where iron particles were deposited onto heated substrates. After Fe RDE-type evaporation, the samples were further annealed at the same temperature for 1–10 min, and then were moved to a cold place inside the vacuum chamber. For comparison, thicker Fe films were deposited onto room temperature Si substrate. Immediately after Fe deposition these layers were annealed in-situ in the vacuum chamber to produce the Fe–silicide. The temperatures were

monitored by small-heat-capacity Ni–NiCr thermocouples.

The following groups of samples were prepared on Si(100) substrates:

- i. 1.5, 3, 4.5, 5, 6, and 8-nm thick Fe films were evaporated by RDE method onto Si(100) substrates kept at 600 °C, and annealed further for 2 min at the same temperature;
- ii. Samples were prepared by RDE method of 5 nm Fe evaporation onto Si at 500 °C, 5 nm Fe onto Si at 600 °C, and 10 nm Fe onto Si at 800 °C. All of the samples were further annealed for 10 min at their preparation temperature, respectively;
- iii. Fe films between 20 and 30 nm thickness were evaporated onto room temperature Si(111) substrates and then annealed at 600 °C for 5 min; and
- iv. 3-nm thick Fe film was evaporated onto Si(100), without any annealing to produce a control sample to see the initial, non-reacted Fe film morphology.

The silicide phases formed were identified by X-ray diffraction using vertical powder diffractometer with a reflected beam monochromator. The thinner samples were measured for a long time to collect data for the extremely weak peaks. The surface morphology of the Fe–silicides was investigated by atomic force microscopy (AFM) and by scanning electron microscopy (SEM). In case of the thick Fe–silicides optical microscopy was used to show the morphology.

## 3. Results and discussion

The AFM scan of the non-reacted Fe film [sample (iv)] did not show any aggregation, the layer seems to be flat without any aggregated island. This means, that the occasional further silicide island formation was not caused by the initial iron distribution.

The properties of the reacted films were investigated first as a function of the thickness at the same short time annealing. After the RDE deposition of the iron films onto Si(100) kept at 600 °C and annealed further for 2 min [sample series (i)], dots are seen in the AFM images. The density of islands increased with the growing thickness, but it was not a linear function of the available amount of Fe. Around 6 nm evaporated Fe thickness, should have been a critical thickness, above, the number of islands suddenly enhanced. These islands are randomly distributed on the surface of the Si(100) substrate. The typical size of an island was in the 20–50 nm range (Fig. 1a,b). According to the extremely weak lines, produced by X-ray diffraction measurements, both  $\alpha\text{-FeSi}_2$  and  $\beta\text{-FeSi}_2$  phases were present in the samples. With the rising thickness of evaporated Fe, the lines of metastable  $\alpha\text{-FeSi}_2$  gradually vanished, and line (002) of  $\beta\text{-FeSi}_2$  became dominant, which indicated an oriented growth.

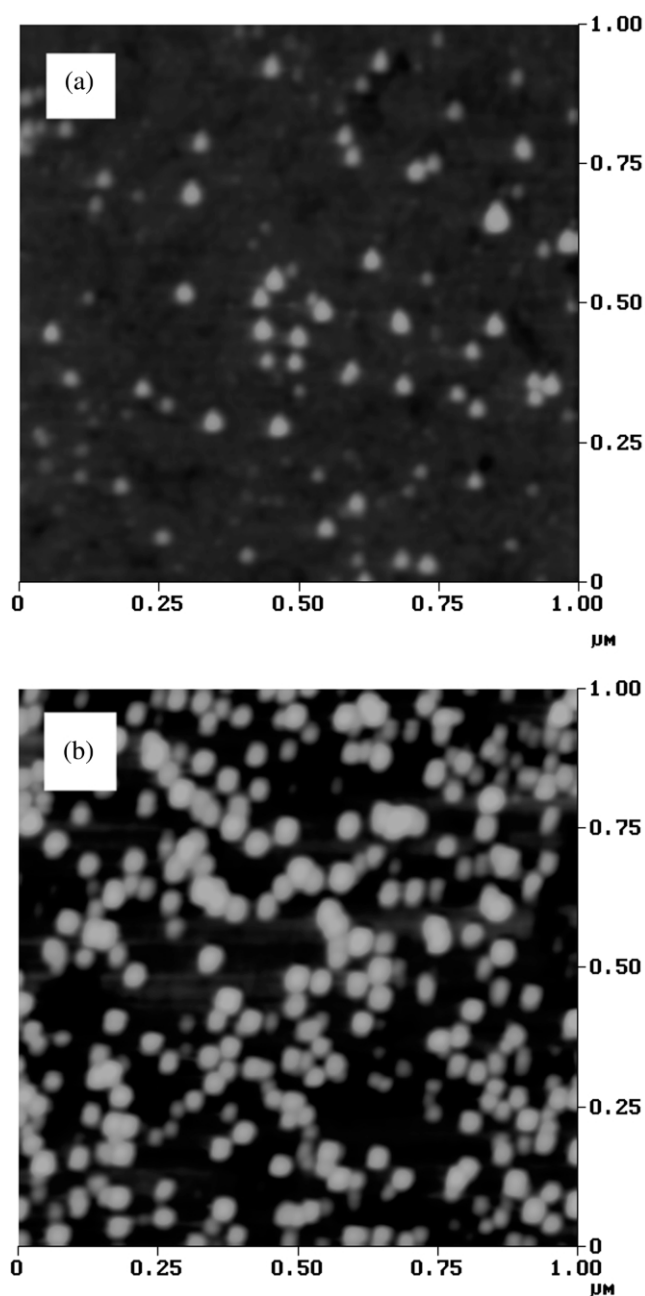


Fig. 1. AFM images of Fe–silicide islands prepared by RDE method at 600 °C and further 2 min annealing from (a) 6 nm (b) 8 nm iron layer.

In case of the second sample series (ii), the duration of the annealing was kept constant after RDE deposition of samples, that had different thickness and annealing temperature. The SEM image of the sample, made by RDE from 5 nm Fe at 500 °C and annealed further at the same temperature for 10 min, can be seen in Fig. 2a. The islands were much bigger than in case of short time annealed samples and their size varied from 50 to 300 nm. The shape of smaller island was typically circular, while the bigger ones had distorted triangular

or quadrangular shapes. The X-ray diffraction pattern measured on this sample is shown in Fig. 3, curve a. The pattern showed that both  $\alpha$ -FeSi<sub>2</sub> and  $\beta$ -FeSi<sub>2</sub> phases were present in this sample.

The higher temperature deposition and annealing (600 °C) of the next sample, with same thickness made radically changed the SEM image (Fig. 2b). The size of aggregated silicides seemed to be similar to the islands of the previous sample, except some rectangular wire like islands, whose length reached 1  $\mu$ m or more. It was interesting, that the rectangular and triangular islands were ordered in specific directions, which were perpendicular to each other according to the Si(100) substrate's cubic lattice. X-Ray diffraction pattern measured on this sample showed sharper lines of  $\alpha$ -FeSi<sub>2</sub> and  $\beta$ -FeSi<sub>2</sub> (Fig. 3, curve b). The separation of these two phases in the pattern was not easy, because the strongest (001) line of oriented  $\alpha$ -FeSi<sub>2</sub> coincided with the (200) line of oriented  $\beta$ -FeSi<sub>2</sub>. To give the estimated rate of the phase quantities from the diffraction results was impossible, since the phases were more or less epitaxial with specific diffraction lines and intensities.

The SEM micrograph of the sample, made by RDE from 10 nm Fe at 800 °C and annealed further at the same temperature for 10 min, can be seen in Fig. 2c. Two form of aggregated Fe–silicide were detected on this sample, the dominant islands were triangularly faceted big (approx. 0.5  $\mu$ m) grains in two directions, and between them smaller nearly circular ones. The X-ray diffraction pattern of this sample contained only two lines namely the (112) and (224) lines of  $\beta$ -FeSi<sub>2</sub>, showing a specially oriented epitaxial relation with Si(100) substrate. It is worth to mention that these lines coincide with the (111) and (222) lines of Fe<sub>3</sub>Si. The solid phase thin film reaction of Fe and Si does not allow the existence of a Fe-rich phase at 800 °C annealing, probably nor in epitaxially stabilized form. However, from geometrical considerations regarding the shapes of the islands, orthorhombic  $\beta$ -FeSi<sub>2</sub> was suggested to be present on the surface of Si(100).

On Fig. 4, can be seen an optical microscopy image of the sample that was evaporated at room temperature with 30 nm Fe and then was annealed at 600 °C for 5 min. According to X-ray diffraction samples contained FeSi and  $\beta$ -FeSi<sub>2</sub> phases. The big  $\beta$ -FeSi<sub>2</sub> nuclei were embedded into the FeSi base layer. It showed that the FeSi  $\Rightarrow$   $\beta$ -FeSi<sub>2</sub> phase transformation is a nucleation-controlled process. The nucleation controlled solid phase reactions produce rough surfaces as a consequence of the coalescence of growing nuclei from different spots. To avoid the rough film morphology, the reactive deposition epitaxy (RDE) method was suggested to prepare thick  $\beta$ -FeSi<sub>2</sub> films also.

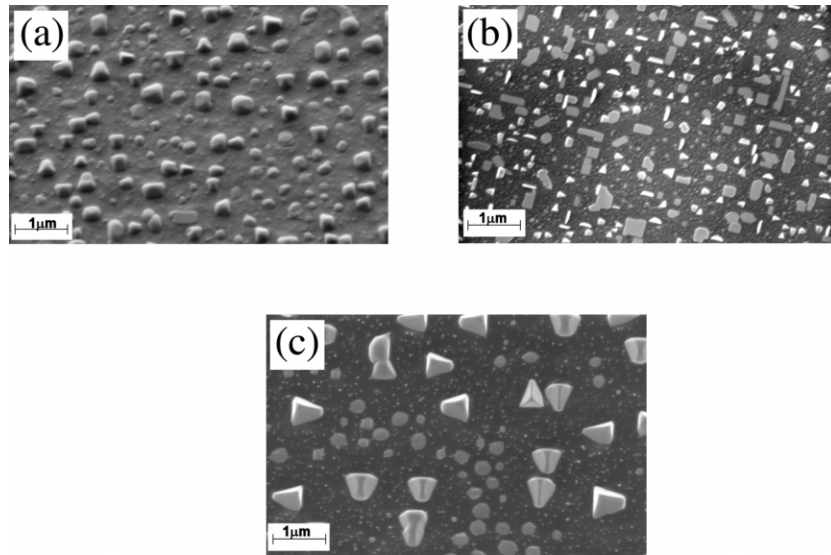


Fig. 2. SEM images of Fe silicide islands prepared by RDE method and further 10 min heat treatment of samples (a) 5 nm Fe and 500 °C, (b) 5 nm Fe and 600 °C, (c) 10 nm Fe evaporation and 800 °C annealing.

#### 4. Conclusion

Iron–silicide islands were grown on Si(100) by reactive deposition epitaxy method and by conventional

solid phase reaction. Self-assembled, island like, oriented  $\beta$ -FeSi<sub>2</sub> and  $\alpha$ -FeSi<sub>2</sub> were found to grow on Si(100) substrates under 15 nm initial Fe thickness. Generally two phases occurred together on samples, and their appearance depended on the evaporated Fe thickness, on the temperature and duration of the annealing. The size of the islands was between 20 and 500 nm, and three main shapes of aggregates appeared: circular to faceted triangular and quadratic. The triangular shape was connected to the specially oriented  $\beta$ -FeSi<sub>2</sub> islands. The circular shape could be occurred at lower temperature annealing and in thinner layers, where the mixed phases had polycrystalline like character. The quadratic shapes were found in samples, where the Fe–silicide

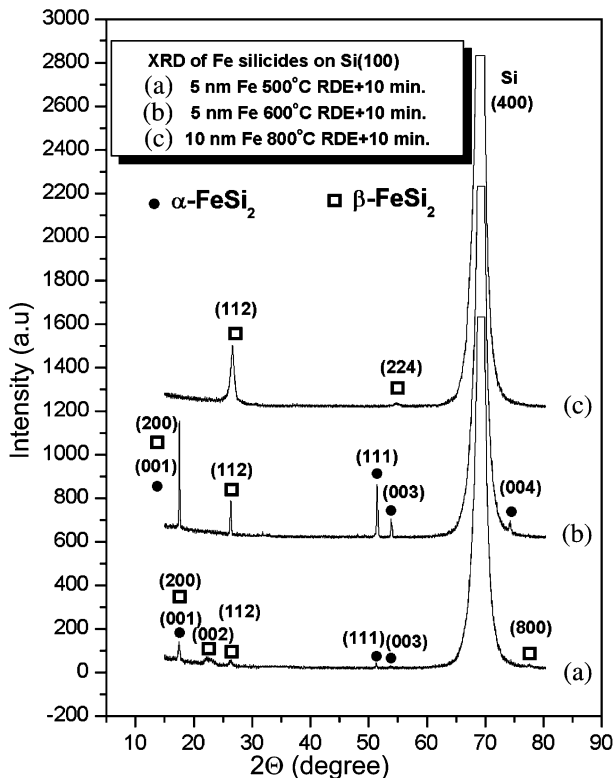


Fig. 3. X-Ray diffraction patterns of Fe silicide islands prepared by RDE method and further 10 min heat treatment of samples (a) 5 nm Fe and 500 °C, (b) 5 nm Fe and 600 °C, (c) 10 nm Fe evaporation and 800 °C annealing.

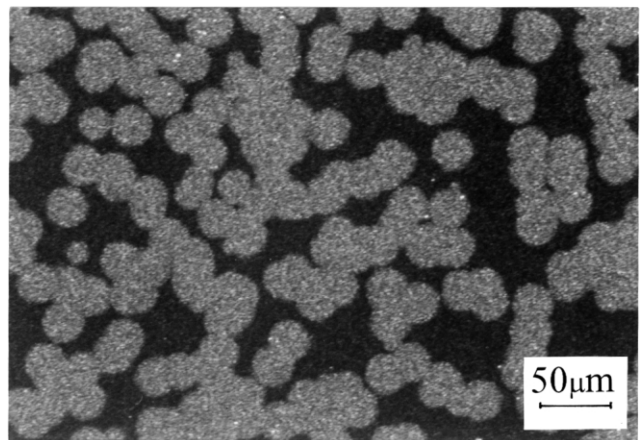


Fig. 4. Optical micrograph of 30 nm evaporated Fe annealed at 600 °C for 5 min. The image shows the FeSi<sub>2</sub> ⇒  $\beta$ -FeSi<sub>2</sub> nucleation controlled solid phase thin film transformation.

phases have rather monocrystalline like structure. Above 20 nm evaporated Fe thickness, the samples show islands of  $\beta$ -FeSi<sub>2</sub> phase grown into the FeSi matrix indicating a nucleation controlled type transition of the FeSi to  $\beta$ -FeSi<sub>2</sub> phase. The separation of  $\beta$ -FeSi<sub>2</sub> islands and their production with homogeneous distribution, and appropriate size, and orientation, needs a lot of experiment to develop epitaxial, semiconductive,  $\beta$ -FeSi islands for Si based optoelectronics.

### Acknowledgments

The authors would like to thank Hungarian Academy of Sciences for partial supporting and of OTKA Grant T030419.

### References

- [1] A.H. Reader, A.H. van Ommen, P.J.W. Weijs, R.A.M. Wolters, D.J. Oostra, Rep. Prog. Phys. 56 (1992) 1397.
- [2] U. Gösele, K.N. Tu, J. Appl. Phys. 53 (1982) 3252.
- [3] F.M. d'Heurle, J. Mater. Res. 3 (1988) 167.
- [4] N.E. Christensen, Phys. Rev. B 42 (1990) 7148.
- [5] D.B. Migas, L. Miglio, Phys. Rev. B 62 (2000) 11 063.
- [6] K. Yamaguchi, K. Mizushima, Phys. Rev. Lett. 86 (2001) 6006.
- [7] H. von Känel, K.A. Mäder, E. Müller, N. Onda, H. Sirringhaus, Phys. Rev. B 45 (1992) 13 807.
- [8] K.A. Mäder, H. von Känel, A. Baldereschi, Phys. Rev. B 48 (1993) 4364.
- [9] N. Jedrecy, A. Waldhauer, M. Sauvage-Simkin, R. Pinchaux, Y. Zheng, Phys. Rev. B 49 (1994) 4725.
- [10] P. Villars, L.D. Calvert, Pearson's Handbook of Crystallographic Data for Intermetallic Phases, Vol. 3, American Society for Metals, Metals Park, OH, 1985.
- [11] L. Jacak, Eur. J. Phys. 21 (2000) 487.
- [12] V.A. Schukin, D. Bimberg, Appl. Phys. A 67 (1998) 687.
- [13] A.L. Barabási, Appl. Phys. Lett. 70 (1997) 2565.
- [14] T.I. Kamins, R.S. Williams, Y. Chen, Y.L. Chang, Y.A. Chang, Appl. Phys. Lett. 76 (2000) 562.
- [15] I. Goldfarb, G.A.D. Briggs, Phys. Rev. B 60 (1999) 4800.
- [16] Y. Chen, D.A.A. Ohlberg, G. Medeiros-Ribeiro, Y.A. Chang, R.S. Williams, Appl. Phys. Lett. 76 (2000) 4004.
- [17] J. Nogami, B.Z. Liu, M.V. Katkov, C. Ohbuchi, N.O. Birge, Phys. Rev. B 63 (2001) 233 305.
- [18] T. Suemasu, M. Tanaka, T. Fujii, S. Hashimoto, Y. Kumagai, F. Hasegawa, Jpn. J. Appl. Phys. 36 (1997) L1225.